COMPONENTS AND PHASES: MODELLING PROGRESSIVE HYDROTHERMAL ERUPTIONS

ROBERT MCKIBBIN[✉,1], THOMASIN A. SMITH[2] and LUKE FULLARD[3]

Abstract

This is a review of progress made since [R. McKibbin, "An attempt at modelling hydrothermal eruptions", *Proc. 11th New Zealand Geothermal Workshop* 1989 (University of Auckland, 1989), 267–273] began development of a mathematical model for progressive hydrothermal eruptions (as distinct from "blasts"). Early work concentrated on modelling the underground process, while lately some attempts have been made to model the eruption jet and the flight and deposit of ejected material. Conceptually, the model is that of a boiling and expanding two-phase fluid rising through porous rock near the ground surface, with a vertical high-speed jet, dominated volumetrically by the gas phase, ejecting rock particles that are then deposited on the ground near the eruption site. Field observations of eruptions in progress and experimental results from a laboratory-sized model have confirmed the conceptual model. The quantitative models for all parts of the process are based on the fundamental conservation equations of motion and thermodynamics, using a continuum approximation for each of the components.

2000 *Mathematics subject classification*: primary 86A99; secondary 76E20, 86A15.

Keywords and phrases: hydrothermal eruptions, boiling in porous media, eruption column.

1. Introduction

Hydrothermal eruptions are phenomena that are known to occur in many geothermal fields around the world. Besides the rare reported physical witnessing of an eruption actually taking place, most evidence is based upon breccia deposits on the surface or the discovery of subsurface formations that record the history of previous eruptions.

Hydrothermal eruptions are categorized as being natural or induced. Natural eruptions include prehistoric and unexploited-field eruptions. In New Zealand,

---

[1]Institute of Information and Mathematical Sciences, Massey University, New Zealand; e-mail: r.mckibbin@massey.ac.nz.
[2]Institute of Fundamental Sciences, Massey University, New Zealand; e-mail: t.a.smith@massey.ac.nz.
[3]Institute of Fundamental Sciences, Massey University, New Zealand; e-mail: l.fullard@massey.ac.nz.

prehistoric eruptions have occurred in Whakarewarewa, Orakeikorako, Rotokawa and other regions of the Taupo Volcanic Zone (TVZ). Waimangu has more recently been an area of interest for large natural eruptions, the latest occurrence being in 1973. The eruption from the crater of Mt Ruapehu on 25 September 2007, with no pre-event seismic warning, may have been of hydrothermal type. Induced eruptions occur as a result of exploitation of geothermal fields. These have taken place in the Tauhara and "Craters of the Moon" areas of the Wairakei Geothermal Field [3].

Such eruptions are violent in nature and can last from a matter of minutes to several hours. A hydrothermal eruption is distinct from a geyser in that the former is noncyclic in occurrence, takes place without warning, and the ejected material is a slushy mixture of water and rock particles of all sizes. These are lifted from the ground by a high-speed jet of gas which is mostly steam, but which could contain noncondensible gases contained in the near-surface water. Most of the material is directed vertically upwards from vents that can be from 5 m to 500 m in diameter; it is then deposited nearby.

The quantitative models which model the mechanical processes to date (see, for example, [5, 9, 17]) are based on the fundamental conservation equations of motion and thermodynamics, using a continuum approximation for each of the components. The first models relied on a simple homogeneous Darcy law to calculate the pressure gradients underground. The effects of adding a nonlinear (Forchheimer) term to the momentum equation were subsequently investigated; numerical experiments revealed this term to be important only when rock permeabilities are relatively large. Some investigation was also made of whether a separated two-phase Darcy law model was better; the rapid process indicates that there is little time either for the dynamic separation of the fluid phases or for heat transfer between the solid and fluid components, and that the simple homogeneous fluid mixture model is appropriate.

The motion of two underground zone boundaries, the "flashing front" and the "erosion surface", has been examined; the two fronts advance downward and use of a quasi-static "snapshot" allows separate estimates to be made of the flashing front speed and the rate of surface erosion. The emerging fluid's speed has been used to estimate the properties of the rising jet, while the flight of the ejected particles has been calculated using recently developed models for dispersion of particles in the air. The three main zones of interest (underground flow, eruption jet and plume dispersion) are now able to be connected to form an approximate, but complete, quantitative model of a hydrothermal eruption.

2. Modelling history

Various authors have investigated the mechanisms of phreatic eruption events. Mastin [8] explored the thermodynamics of boiling-point, gas, and hot water-rock eruptions, concluding that the boiling-point eruptions were likely to be larger and of longer duration than the gas and hot water-rock eruptions. Germanovich and Lowell [6] discussed mechanisms for eruptions related to magmatic intrusion into water-saturated permeable rock, and [23] studied explosive volcanic phenomena.

Geyser theory and modelling was researched in [7]. A review of current hydrothermal eruption knowledge around the world is provided in [4].

The earliest attempts at modelling the mechanical processes of hydrothermal eruptions were explored in [9]. Speculation as to the initiating event had been based around the idea of a small seismic motion that disturbed latently unstable conditions near the surface. The causes of the instability were supposed to be one of three types: the first was formation of a steam cap due to a drop in groundwater level with increased steam-flow to the surface; the second was hydraulic fracturing and brecciation allowing noncondensible gases to decrease water boiling pressures; and the third was a reduction in lithostatic pressure caused by lifting of overburden material.

A discussion of these proposed mechanisms was given in [9]. In particular, the type of eruptions classified as "hydrothermal" would preclude any large-scale "blast". The process is started near the surface, and the greatest effect is when the near-surface fluid is liquid, as that provides the greatest potential for expansion and high fluid ejection speeds. A steam cap provides small expansion potential; that and the presence of noncondensible gases were explored in [11], where it was found that very large over-pressures of a gas such as CO_2 would be required to have any significant effect over that of pure water. Further, the potential of deeper overburden-lifting pore pressures to produce significant upward movement of large ground masses would be reduced by any escape of fluid which would immediately reduce the lifting force.

Conclusions from these and other considerations have led to the view that a progressive hydrothermal eruption proceeds due to boiling of near-surface fluid, with liquid water providing the greatest potential for removal of ground-surface breccia. The expansion potential of such water can be expressed in terms of the "specific volume ratio" which compares the density of the fluid in the ground with that of the same mass when expanded to ambient atmospheric conditions [10, 11]. The greatest values are for liquid groundwater, while any steam fraction there considerably reduces the potential. An investigation of the presence of noncondensible gases [11] indicated that these have less effect in regions where the gas saturation is low. It is concluded from the combination of these investigations that noncondensible gases such as CO_2 may be neglected, and that near-boiling-point liquid water is most likely to produce effective eruptions. The concept is based on mining by steam lifting, rather than by sudden explosions such as those caused by phreatomagmatic phenomena. Browne and Lawless [4] consider this the most common cause of hydrothermal phenomena.

The lift caused by the motion of the boiling fluid escaping upwards to the atmosphere has to exceed the weight of rock particles at the ground surface as well as any cohesive forces that are binding them together. The latter were taken account of by [1, 2, 9, 10]. An appropriate model for the movement of the boiling fluid was the subject of extensive investigation as reported by [17–22]. The rapid process and high speed of the upwardly moving fluid leads to the conclusion that there is little time for thermodynamic equilibration between the fluid and the rock matrix, or for dynamic separation of the two fluid phases. At most, the fluid state is controlled by the

condition that the fluid is at saturated conditions and it flows as a two-phase boiling mixture, with negligible heat transfer between it and the solid matrix (that is, adiabatic flow). The fluid mass transfer is therefore modelled as isenthalpic.

In the earliest modelling attempts, when the flow above the ground was less well understood, it was supposed that conditions there were akin to a fluidized bed. Examination of reports of the (rare) field observations and photographs, as well as some of the volcanological literature, led to the concept that the rock particles were mere "passengers" within the rising jet of gas-dominated fluid, as indeed were the water droplets, and that the early model was incorrect. The rock particles and droplets form an extremely small volume fraction of the jet. While the water droplet mass increases due to condensation as the hot fluid mixture entrains cold air, the liquid phase still forms a very small volumetric fraction in the plume above the ground.

Investigations of the form of the jet based on considerations of these concepts were reported in [14–16]. The subsequent dispersion and deposition of the ejecta have been based on recently developed models for particle transport by the atmosphere [12, 14]. These models allow for agglomeration of wet particles, but do not allow specifically for evaporation of the water after release from the eruption jet. Models incorporating the latter phenomenon are under current investigation by the first author and other colleagues.

Quiescent conditions after the eruption has taken place were considered by [17], who modelled the subsequent groundwater flow near the event as the system "recovered" to a new pre-eruptive state. The almost incompressible liquid groundwater flow is controlled immediately by surrounding pressures, with conductive and/or convective heat flow following much more slowly.

Below is a brief summary of the mathematical models used for the various parts of hydrothermal eruptions, using the assumptions and simplifications as outlined above.

3. Below ground

The main driving force of hydrothermal eruptions is supposed to be an increased pressure gradient immediately below the surface of the ground arising from the fluid near the surface being suddenly exposed to atmospheric conditions. In order for a particle of rock at the surface to be moved, the equilibrium of forces that govern the static particle rock matrix must be upset.

In summary, it is supposed that hot fluid, initially at rest in the rock matrix, begins to escape to the atmospheric conditions at the surface, flashing (boiling) and increasing in specific volume as the pressure decreases. The increasing speed of the two-phase fluid as it nears the surface provides lift to the rock particles. A hydrothermal eruption can take place when the fluid speed is great enough to eject the particles, that is, the hydrodynamic lift is large enough to overcome the effective weight and cohesive stresses (if any) of the rock particles. The eroding surface and the flashing front in the formation are both considered to be moving boundaries. Assumptions made in the authors' model are as follows.

(1) The principles of conservation of mass, momentum and energy hold.
(2) The fluid below the flashing zone is motionless.
(3) The flowing fluid is a homogeneous mixture of liquid water and steam—it is assumed that, because boiling occurs very quickly, the two phases flow at the same speed.
(4) The moving fluid is at saturated (boiling) conditions.
(5) The process is quasi-steady, that is, the eruption has already been initiated and is currently in progress, and is modelled as being, albeit for short time periods, nearly steady.
(6) The fluid lifts the rock particles at the surface, where conditions are atmospheric ($p = 1$ bar abs.).
(7) Thermal conduction is ignored, that is, there is negligible heat transfer between the fluid and rock in the flashing zone – the process is modelled as being adiabatic, and the fluid flow is isenthalpic.

There are two moving boundaries to the flashing zone where underground fluid movement is taking place. The lower boundary, termed the "flashing front", propagates downward into the stationary fluid in the rock matrix at speed V. The boundary formed by the eroding ground surface above also propagates downward; its speed is V_{er}. The early models assumed that $V_{er} = V$ but this is not justifiable, nor is it necessary for the calculations to be carried out.

The flashing front moves downward at speed V into a fluid-filled medium of porosity ϕ and permeability k where the fluid has liquid saturation S_{ld} (volume fraction of liquid in the two-phase fluid), vapour saturation $S_v = 1 - S_l$, mixture density ρ_{fd}, and mixture specific enthalpy h_{fd}, all of which may vary with depth (parameters concerned with conditions at depth have a d subscript whilst those associated with conditions at the top (eroding) surface, where $p = 1$ bar abs., have a t subscript). The average fluid particle (pore) velocity is V_f. Subscripts f, r, l and v denote fluid, rock, liquid water and vapour (water gas), respectively.

The technique is to refer all moving quantities to a frame of reference that moves downward at the same speed V as the flashing front (see Figure 1). Because the motion is assumed to be quasi-steady, the frame of reference can be treated as inertial for the short periods of time considered. Within this frame, the flow is assumed steady.

3.1. Conservation of mass   The flashing front moves into a motionless fluid in the pores of the medium. The (constant) fluid mass flowrate per unit area m_f through this region and the flashing zone, relative to the moving frame of axes (Figure 1), is

$$m_f = \phi \rho_f (V + V_f), \tag{3.1}$$

but at the "flashing front" $V_f = 0$, hence

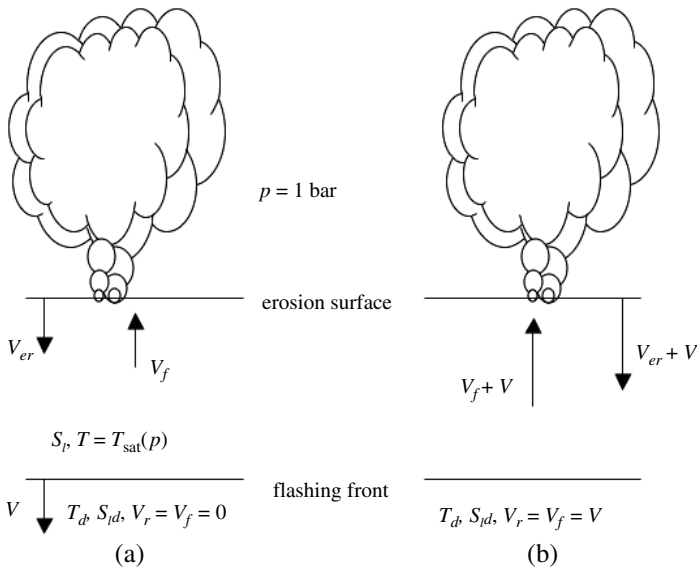$$m_f = \phi \rho_f (V + V_f) = \phi \rho_{fd} V. \tag{3.2}$$

FIGURE 1. Schematic of flows: (a) relative to fixed axes; (b) relative to a frame of reference moving downwards with the flashing front.

The fluid mixture densities are

$$\rho_f = S_l\rho_l + (1 - S_l)\rho_v,$$
$$\rho_{fd} = S_{ld}\rho_{ld} + (1 - S_{ld})\rho_{vd}. \tag{3.3}$$

3.2. Conservation of momentum The fluid volume flowrate per unit area, w_f, relative to the fixed frame of axes is given by using the simple Darcy law for the motion of the homogeneous two-phase fluid mixture:

$$w_f = \frac{k}{\mu_f}\left(-\frac{dp}{dz} - \rho_f g\right). \tag{3.4}$$

For the boiling mixture, the dynamic viscosity is here taken to be

$$\mu_f = \mu_l^{S_l}\mu_v^{S_v} = \mu_l^{S_l}\mu_v^{1-S_l} \tag{3.5}$$

but other correlations are possible. With the assumption that the boiling fluid is moving as a homogeneous two-phase mixture, the corresponding liquid and vapour mass flowrates per unit area relative to the moving axes are $m_l = S_l\rho_l(w_f + \phi V)$ and $m_v = (1 - S_l)\rho_v(w_f + \phi V)$ and the total mass flow per unit area is $m_f = m_l + m_v = \rho_f(w_f + \phi V)$.

Equation (3.1), after rearrangement and use of (3.4) gives

$$V_f = \left(\frac{\rho_{fd}}{\rho_f} - 1\right)V = \frac{k}{\phi\mu_f}\left(-\frac{dp}{dz} - \rho_f g\right), \tag{3.6}$$

which can be rearranged to give an expression for the local pressure gradient:

$$\frac{dp}{dz} = -\rho_f g - \frac{\mu_f \phi V}{k}\left(\frac{\rho_{fd}}{\rho_f} - 1\right). \tag{3.7}$$

From (3.2) it can also be deduced, by applying the surface boundary conditions, that

$$V = \frac{V_{ft}}{(\rho_{fd}/\rho_{ft}) - 1} = \frac{V_{ft}}{(v_{ft}/v_{fd}) - 1} \tag{3.8}$$

where v is the specific volume. This equation relates the flashing front speed to the speed and density of the fluid as it reaches the surface. The overall volume expansion factor for the flashing fluid as it rises from the bottom to the surface is given by

$$v_{\text{rat}} = \frac{v_{ft}}{v_{fd}} = \frac{\rho_{fd}}{\rho_{ft}}. \tag{3.9}$$

3.3. Conservation of energy The vertical energy flux per unit area associated with the fluid flow, relative to the fixed frame of axes, is given by

$$q_e = m_l h_l + m_v h_v = m_f h_f \quad \text{where} \quad h_f = \frac{\rho_v h_v(1 - S_l) + S_l \rho_l h_l}{S_l \rho_l + (1 - S_l)\rho_v} \tag{3.10}$$

is the so-called "flowing enthalpy" of the fluid. Boundary conditions at the flashing front give

$$q_e = m_f h_{fd}.$$

Because q_e is conserved and m_f is constant, $h_f = h_{fd}$ and the fluid flow is isenthalpic; the constant value of the specific enthalpy is given by that at the flashing front:

$$h_{fd} = \frac{\rho_{vd} h_{vd} + S_{ld}(\rho_{ld} h_{ld} - \rho_{vd} h_{vd})}{\rho_{fd}}.$$

Rearrangement of (3.10) gives the liquid saturation in terms of the specific enthalpies and densities of the phases:

$$S_l = \frac{\rho_v(h_v - h_f)}{(\rho_l - \rho_v)h_f + (\rho_v h_v - \rho_l h_l)}. \tag{3.11}$$

3.4. Equation of state The fluid is assumed to be at saturated (boiling) conditions and the equation of state is

$$p = p_{\text{sat}}(T) \quad \text{with} \quad \left(\frac{dp}{dT}\right)_{\text{sat}} = \frac{h_v - h_l}{(v_v - v_l)(T + 273.15)}$$

where temperature T is measured in degrees Celsius.

3.5. Lift condition The condition that a rock particle be lifted off the ground surface is related to the hydrodynamic lift at the surface, given in terms of the relative speed of the fluid with respect to the rock by

$$L_t = \frac{3}{4} C_{ds} \frac{1-\phi}{\phi \phi_s d_p} \rho_{ft} |V_{ft} - V_r| (V_f - V_r) \tag{3.12}$$

where $\phi_s = 1.0$ for spheres and $C_{ds} = 0.38$ for Re ≥ 1500 [9]. Assuming no *in situ* cohesive stresses, the criterion that the dynamic lift exceeds the effective weight of the rock (that is, the net lift is positive) is given by

$$L_t - \phi(1-\phi)(\rho_r - \rho_{ft})g > 0. \tag{3.13}$$

The most important parameter of interest is the fluid particle velocity at the ground surface. This is found by considering the lift condition (3.12) and (3.13). With the knowledge that just below the eroding surface $V_r = 0$, and that V_f is to be determined just at the point where the net lift is zero, substituting (3.12) into (3.13) with equality and rearranging gives

$$V_{ft} = \sqrt{\frac{4\phi^2 \phi_s d_p}{3 C_{ds}} \left(\frac{\rho_r}{\rho_{ft}} - 1 \right) g}. \tag{3.14}$$

Given the temperature of the fluid at the flashing front, the bottom boundary conditions are determined using correlations to find the pressure (at saturated conditions), densities, and enthalpies. The surface is assumed to be at atmospheric pressure. Equation (3.9) provides the volume expansion factor v_{rat} and the flashing front speed V may be found using (3.8).

The Reynolds number for the flow as the fluid emerges at the surface is given by

$$\mathrm{Re}_t = \frac{\rho_{ft} d_p V_{ft}}{\mu_{ft}}. \tag{3.15}$$

Numerical results [1, 2, 10] show that, for a reservoir temperature above 100 °C, the maximum fluid expansion occurs when $S_{ld} = 1$; the flashing front speed also appears smallest for $S_{ld} = 1$. Reynolds numbers for any liquid saturation are of the order of at least 100 000. One of the major benefits of using the lift force balance (3.13) for determining V_{ft} was provision of an estimate of the thickness of the flashing zone. Some interesting qualitative information resulted for particular experimental cases.

3.6. Modification for cohesive stresses The properties of the fluid as it makes its way to the surface are traced by integration of (3.7). At each step of the integration, the lift condition (3.13) is tested. If a nonzero *in situ* cohesive stress is allowed for, the criterion for a particle to be lifted is

$$L_t - \phi(1-\phi)(\rho_r - \rho_{ft})g > \text{cohesion}. \tag{3.16}$$

3.7. Fluid properties Correlations for the fluid thermodynamic properties for near sub-surface conditions can be found in [17]. Since the temperature of the fluid which is involved in an eruption is unlikely to exceed 150 °C, these will be accurate enough for the modelling required here.

4. Advancement to higher dimensions

The work and results of this section are new and are a result of investigations in [5]. Equations (3.6) and (3.7) can easily be converted to polar coordinates:

$$V_f = \left(\frac{\rho_{fd}}{\rho_f} - 1 \right) V = \frac{k}{\phi \mu_f} \left(-\frac{dP}{dr} - \rho_f g \sin \theta \right), \qquad (4.1)$$

$$\frac{dP}{dr} = -\rho_f g \sin \theta - \frac{\mu_f \phi V}{k} \left(\frac{\rho_{fd}}{\rho_f} - 1 \right). \qquad (4.2)$$

The above can be integrated as before, but with our moving reference frame in the radial direction, that is, V and V_f are now radial velocities. The angle θ is taken such that $\theta = 0$ is the horizontal ground surface, and $\theta = \pi/2$ is vertical. This provides a 2D model and, by symmetry (rotation about the z-axis), a 3D model.

4.1. 2D model The behaviour of various parameters at various angles in the 2D model has been investigated and discussed in detail in [5]. The analysis showed a greater flashing front velocity V for angles θ closer to zero, but a smaller fluid velocity V_{ft}. The model also yielded an "almost" power law relationship for the rate of change of both velocities. The shape of the (initially semi-circular) crater was also found to expand both in width and depth, but the expansion in width was greater than the deepening of the crater. Further analysis can be found in [5].

4.2. Reynolds numbers A key parameter in (3.15) is the rock particle diameter d_p. Not only does the Reynolds number depend explicitly on d_p by (3.15), but also implicitly since V_{ft} is proportional to $\sqrt{d_p}$ by (3.14). This implies that a reduction of d_p by a factor of ten should reduce the Reynolds number by a factor of 0.0316. Figure 2 contains plots of the Reynolds number and fluid velocity at various points on the surface for cohesive stress = 5000 Pa m^{-1}, and $d_p = 0.1$ m, 0.01 m and 0.001 m, respectively.

Figure 2 displays the angular dependence of the Reynolds number and the fluid velocity. Large values of d_p result in turbulent flow (Re > 3000). Lowering d_p brings us closer to laminar flow, and in fact, for $d_p = 0.001$ m, all of the flow is in the laminar region. Also, the Reynolds number decays much faster than for the smaller d_p values.

The decay of the Reynolds number (after the large peak) implies that viscous forces are becoming more important in the flow (as opposed to inertial forces). Presumably at some time in the future the viscous forces will become so dominant that the eruption will slow or even cease. Therefore a possible mechanism for termination of an eruption could be the inertial to viscous force ratio.
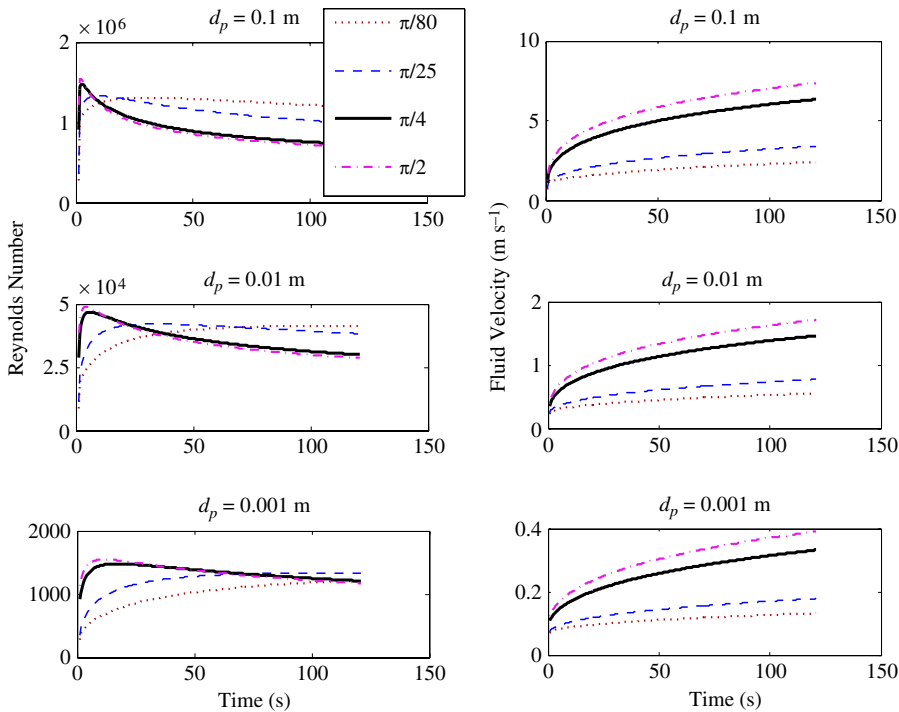
FIGURE 2. Reynolds number and fluid velocity plots. Cohesive stress $= 5000\ \mathrm{Pa\ m^{-1}}$.

The higher values of the Reynolds number for the larger d_p values indicate that larger rock particles displaced by the fluid rising during an eruption cause the fluid to flow turbulently around them, but small rock particles (small d_p values) of order 1 mm in diameter may allow surrounding fluid to flow in a laminar fashion. Also, the quicker decay of the Reynolds number for larger values of d_p indicates that the eruption of larger rocks may not persist as long as the eruption of smaller material. In effect, the eruption may begin ejecting mixtures of large and small material, but as the eruption evolves, only smaller and smaller material is ejected, until the eruption ceases.

The above observations may help in bridging the gap between the below and above ground flow models.

5. The motion of the upper boundary

Bercich and McKibbin [1, 2] describe the process for finding the downward speed of the erosion surface. Given conditions at the flashing front, the pressure gradient (3.7) is integrated upwards until the lift criterion is satisfied.

In detail, given a value of V and a state point $(T,\ p_{\mathrm{sat}}(T))$ in the flow, evaluation of the thermodynamic properties from correlations allows calculation of S_l

from (3.11), μ_f from (3.5), ρ_f from (3.3) and hence the local pressure gradient from (3.7). Integration of (3.7) from the flashing front upwards allows testing of the lift condition (3.16) at the point where $p = 1$ bar abs. (the ground surface). The value of flashing front speed V can be adjusted until the lift condition is exceeded; this will then give the flashing zone thickness.

A small increment in time allows the new position of the flashing front, and hence the thermodynamic conditions there, to be determined from the initial temperature and saturation profiles underground. The process is repeated; the positions of the flashing front and erosion surface are then found as functions of time.

Can this process be used to trace the motion forward through time and find any reason why it might eventually stop? Can one then go "back in time" and glean some information about the phenomenon's initiation?

6. The eruption jet

A by-product of the above method is the time-dependent structure of the fluid stream that issues from the ground, as well as the volume erosion rate. The first of these may be used as surface boundary conditions for the fluid in the eruption jet. Given a particle size distribution in the ground, the volume erosion rate allows the (uncoupled) problem of particle ejection to be calculated. This part of the process was formulated and described by [12, 15].

The main features of this part of the model are the initial composition and speed of the emerging two-phase fluid stream and the entrainment of air into the jet. Conservation laws allow a simple one-dimensional model for the jet, which is supposed to be approximately circular. It is supposed that the pressure within the jet is close to atmospheric, with contributions of partial pressures from the entrained air and the water vapour. As the jet rises, it cools and some of the vapour condenses to satisfy the thermodynamic requirement of saturated conditions for the water component. Calculations suggest that the jet increases in diameter until it becomes infinitely wide at a certain height, the top of the jet, where the upward velocity becomes zero; the speed of the jet decreases almost linearly with height above the ground. As the speed decreases with elevation, so too does its ability to lift the entrained particles, which are then released to fall and be deposited on the ground.

Because the jet slows with increasing elevation, any particle that leaves the surface must have previously been restrained from doing so by some cohesive force. If not, the lift criterion will not be exceeded immediately above the ground and the particle will not be elevated further. While small particles that are initially bound by cohesion become detached and accelerate upwards until the jet can no longer support them, larger clasts that are not cohesively attached, or that do not shed smaller fragments, might not leave the erosion surface but just remain close to the ground. They would descend into the eruption crater as smaller particles are swept away upwards past them. The eruption therefore may act as a size-sorting mechanism for the particles.

The geometry of the flow models is that of a column of circular horizontal cross-section with a vertical axis (see Figure 3). The vertical fluxes are based on the average
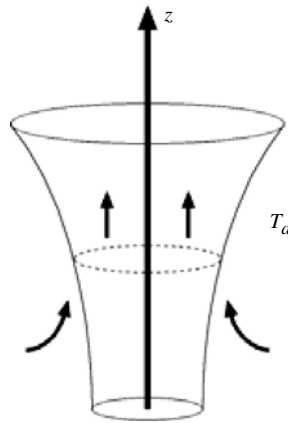
FIGURE 3. Diagram illustrating the geometry of the flow.

vertical speed of the fluid. Where there are multiple components (liquid water, water vapour, and air) it is assumed that their speeds are the same, that is, they are well mixed.

The model is of a moving column (jet) of a steam-dominated mixture of water vapour and liquid water droplets that issues from the ground from a circular region of radius r_0. As the fluid rises, it entrains air from the surrounding atmosphere, at ambient temperature T_a.

The resulting jet rises vertically and grows in radius, $r(z)$, at height z above ground level at $z = 0$, with $r(0) = r_0$. It is assumed that the flow is at steady state for a short period of time. As air is entrained into the flow, the total vertical mass flux $M(z)$ increases from $M(0) = M_0$ to $M(z) > M_0$ due to air entrainment. The total water flow (liquid and vapour) remains constant (M_w) while the air flow (M_a) increases with z. The total mass flow is $M = M_w + M_a$.

The mass fraction of water per unit volume (X_w) decreases from $X_w(0) = 1$ as z increases. That for air ($X_a = 1 - X_w$) increases from $X_a(0) = 0$ as z increases.

The liquid mass fraction of the water flux is Y_l, that of vapour is Y_v and $Y_l + Y_v = 1$. So $M_l = Y_l M_w = Y_l X_w M$ and $M_v = Y_v M_w = Y_v X_w M$. The total gas flow (which provides the lift for the particles) is then given by

$$M_g = M_v + M_a = Y_v X_w M + X_a M = \left(Y_v + \frac{1 - X_w}{X_w} \right) M_w.$$

6.1. Mass conservation Conservation of mass requires that the vertical rate of mass increase in the column is equal to the mass entrainment rate around the column surface:

$$\frac{dM}{dz} = \frac{dM_a}{dz} = 2\pi r \rho_{\text{atm}} E(w), \tag{6.1}$$

where the upwards mass flux within the column is

$$M = M_l + M_v + M_a = \rho \pi r^2 w.$$

Here, $r(z)$ is the radius of the column (circular cross-section of the flow), $w(z)$ is the mean vertical speed in the flow, and $\rho(z)$ is the density of the fluid flow given by $\rho = \rho_l + \rho_v + \rho_a$ with each component contributing a partial pressure to the total pressure p_{atm}, the ambient pressure. It is assumed that the pressure within the column is the same as in the surrounding air and therefore that $\rho = \rho_{\text{atm}}$. Note that the density of the air component of the stream is not the same as the atmospheric density, since the air component in the jet is at a reduced partial pressure.

$E(w)$ is the volume entrainment rate per unit surface area of the column, modelled here by

$$E(w) = k w \left(\frac{w_0}{w} \right)^n$$

with constant dimensionless parameters k and n. The fluid mass flux issuing from the ground is given by $M_0 = \rho_0 \pi r_0^2 w_0$, where the subscript 0 indicates values at $z = 0$.

6.2. Momentum conservation   The surrounding air that is being entrained has zero vertical momentum initially. The momentum of the flow is reduced by gravitation and by the effective inertia of the entrained gas; since it is assumed that the pressure in the column is uniform and the same as the surrounding atmosphere, there is no pressure work. The resulting equation is

$$\frac{d}{dz}(Mw) = -\rho \pi r^2 g. \tag{6.2}$$

6.3. Energy conservation   The energy equation takes into account changes in the kinetic and internal energy of the flow components:

$$\frac{d}{dz} \left(\frac{1}{2} M w^2 + M_l u_l + M_v u_v + M_a u_a \right) = -\rho \pi r^2 g w + \frac{d M_a}{dz} u_{\text{atm}}, \tag{6.3}$$

where the u_i are the specific internal energies of the various fluid components.

Since the water mass flux M_w is constant, it is useful to use X_w, the mass fraction of the water in the flow, defined by $M_w = X_w M$. This means that the air mass fraction is $M_a = X_a M = (1 - X_w) M$. Substitution into (6.1) and (6.2) and some rearrangement gives

$$\frac{dX_w}{dz} = -2\pi r \frac{X_w^2}{M_w} \rho_{\text{atm}} k w \left(\frac{w}{w_0} \right)^n, \quad \frac{dw}{dz} = -\frac{X_w}{M_w} \left[\rho \pi r^2 g + k w^2 \left(\frac{w}{w_0} \right)^n \right]. \tag{6.4}$$

Some simplification of (6.3) involving use of the Appendix A formulae gives

$$\frac{dT}{dz} = -\frac{w^2/2 - c_a(T - T_{\text{atm}})}{[X_w c_w + (1 - X_w) c_a] X_v} \frac{dX_w}{dz}. \tag{6.5}$$

7. Results

Numerical integration of the three coupled ordinary differential equations (6.4) and (6.5) gives results with the following general features: the radius of the column increases with height as the flux increases due to entrainment, while the jet speed decreases due to gravitational and inertial slowing; the radius diverges to an infinitely large value as the speed drops to zero. For further results and analysis, see [15].

8. Flight of the ejecta

In general, as discussed above, only small particles that have broken away from heavier clasts are able to be ejected by the emerging fluid stream. Heavier particles remain at ground level, jostled by the lower parts of the jet. The small particles are accelerated upwards until their weight equals the lift afforded by the decelerating column, when they are released into the surrounding air and are then moved by any cross-flow (wind) near the jet. The model for this part of the eruption is that of an advection–dispersion mechanism where the forces correspond to wind drag, gravitational settling and turbulence of the wind flow. The particles will be released at different levels according to their size, with smaller ones lifted to higher levels.

The components in this part of the model are small rock particles, water droplets and air. It is assumed here that the air-flow is not affected by the jet, and that the water droplets are neglected once they leave the upflow. The focus is therefore on the cohort of solid particles that is transported by the forces listed above, according to the advection–dispersion (sometimes called the convection–diffusion) equation. For simplicity, this is stated here for a mass Q_S of particles of a certain size with a corresponding free-air settling speed (terminal speed) S, released into a wind with horizontal speed U, and with turbulent dispersion coefficients $D_L = U L_L$ and $D_T = U L_T$ in the down- and cross-wind directions respectively, where L_L and L_T are the corresponding dominant length scales of the turbulence of the flow. The wind-flow parameters generally vary with elevation above the ground. The mass density (mass per unit volume of air) of the particles is denoted $c(x, y, z, t)$, in Cartesian coordinates, where the x-axis is aligned to the downwind direction. The particles are supposed to be released at point $(0, 0, H)$ a distance H above the jet source, which is approximated by the point $(0, 0, 0)$. The corresponding equation is

$$\frac{\partial c}{\partial t} + U \frac{\partial c}{\partial x} - S \frac{\partial c}{\partial z} = D_L \frac{\partial^2 c}{\partial x^2} + D_T \frac{\partial^2 c}{\partial z^2} + Q_S \delta(x)\delta(z - H)\delta(t). \quad (8.1)$$

Results from calculations where the atmosphere is modelled as a layered system were described in [12] in the context of fallout of particles and droplets from a hydrothermal eruption. Equation (8.1) then applies in each layer where the wind speed and turbulence characteristics and the settling speed are considered constant, but possibly different from those in other layers. Inclusion of a forest canopy, where the particles may be trapped by foliage, was considered for the more general case of transport of solid particles such as pollen, dust, sand, volcanic ash, and so on, by [13].

The transport of ejecta from a hydrothermal eruption is found by regarding the solution of (8.1) as a basic building block. Different-sized particles will have different settling speeds S, corresponding release heights H found from the eruption jet dynamics, and different associated cohort masses Q_S depending on the material mix that is ejected. The solutions for all sets of parameters may be found as a linear combination of the component cohorts. Because the solution to (8.1) may be found in closed form [13], computation is straightforward.

However, while the solution may be used to estimate the flight and deposition of ejected particles for any given eruption, it relies on some knowledge about the size composition of the ejected material. Historical data from typical areas (such as "Craters of the Moon", Wairakei, where deposits have been analysed) could be used, but the role of liquid water in the joining of small particles into larger-sized agglomerates may be difficult to model. This aspect, which also applies to volcanic ashfall as well as the dust–sand–water mixtures of hydrothermal eruptions, is the subject of continuing investigation.

9. Summary and conclusions

The above is a summary of progress to date in the modelling of the various physical processes involved in hydrothermal eruptions.

Appendix A. Thermodynamic variables

Densities

$$\rho_v = p_v/461.527/T \text{ kg m}^{-3}$$
$$\rho_a = p_a/287.099/T \text{ kg m}^{-3}$$

Internal energies

$$u_v = 2375 \times 10^3 + c_v(T - 273.15) \text{ J kg}^{-1}$$
$$c_v = 1310 \text{ J kg}^{-1} \text{ K}^{-1}$$
$$u_a = c_a(T - 273.15) \text{ J kg}^{-1} \quad c_a = 1010 \text{ J kg}^{-1} \text{ K}^{-1}$$

References

[1]   B. J. Bercich and R. McKibbin, "Modelling the development of natural hydrothermal eruptions" (corrigendum), *Proceedings of the 14th New Zealand Geothermal Workshop 1992* (University of Auckland, 1992), 305–312.

[2]   B. J. Bercich and R. McKibbin, "Modelling the development of natural hydrothermal eruptions", *Proceedings of the 15th New Zealand Geothermal Workshop 1993* (University of Auckland, 1993), 345–346.

[3]   P. F. Bixley and P. R. L. Browne, "Hydrothermal eruption potential in geothermal development", *Proceedings of the 10th New Zealand Geothermal Workshop 1988* (University of Auckland, 1988), 195–198.

[4]   P. R. L. Browne and J. V. Lawless, "Characteristics of hydrothermal eruptions, with examples from New Zealand and elsewhere", *Earth Science Reviews* **52** (2001) 299–331.

[5]   L. Fullard, "Hydrothermal eruption model in 2 and 3 dimensions", Honours Project, Massey University, Palmerston North, New Zealand, November 2007.

[6]   L. N. Germanovich and R. P. Lowell, "The mechanism of phreatic eruptions", *J. Geophys. Res.* **100** (1995) 8417–8434.

[7]   K. M. Luketina, "The history and application of geyser theory", Post-graduate Diploma of Science Dissertation, Auckland University, 1996.

[8]   L. G. Mastin, "Thermodynamics of gas and steam-blast eruptions", *Bull. Volcanology* **57** (1995) 85–98.

[9]   R. McKibbin, "An attempt at modelling hydrothermal eruptions", *Proc. 11th New Zealand Geothermal Workshop 1989* (University of Auckland, 1989), 267–273.

[10] R. McKibbin, "Mathematical modelling of hydrothermal eruptions", *Geothermal Resources Council Transactions* **14** (1990) 1309–1316. (Presented at 1990 International Symposium on Geothermal Energy.)

[11] R. McKibbin, "Could non-condensible gases affect hydrothermal eruptions?", *Proceedings of the 18th New Zealand Geothermal Workshop 1996* (University of Auckland, 1996), 323–330.

[12] R. McKibbin, "Modelling deposition of hydrothermal eruption ejecta", *Conference Proceedings: New Zealand Geothermal Workshop & NZGA Seminar*, 15–17 November 2006 (University of Auckland, 2006).

[13] R. McKibbin, "Modelling pollen distribution by wind through a forest canopy", *JSME Internat. J. Ser. B* **49** (2006) 583–589.

[14] R. McKibbin, L. L. Lim, T. A. Smith and W. L. Sweatman, "A model for dispersal of eruption ejecta", *Proc. World Geothermal Congress 2005*, Antalya, Turkey (International Geothermal Association, 2005). Paper no. 0715. ISBN 975-98332-0-4.

[15] R. McKibbin and T. A. Smith, "Hydrothermal eruption jets: air entrainment and cooling", *Conference Proceedings: New Zealand Geothermal Workshop & NZGA Seminar*, 15–17 November 2006 (University of Auckland, 2006).

[16] P. R. Rynhart, R. McKibbin and D. R. Kelly, "Modelling the flight of hydrothermal eruption ejecta", *Proceedings of the 22nd New Zealand Geothermal Workshop 2000* (University of Auckland, 2000), 189–195.

[17] T. A. Smith, "Mathematical modelling of underground flow processes in hydrothermal eruptions", Ph. D. Thesis, Massey University, Palmerston North, New Zealand, 2000.

[18] T. A. Smith and R. McKibbin, "Modelling of hydrothermal eruptions: a review", *Proc. 19th New Zealand Geothermal Workshop 1997* (University of Auckland, 1997), 123–128.

[19] T. A. Smith and R. McKibbin, "Towards a hydrothermal eruption model", *Proceedings of the 20th New Zealand Geothermal Workshop 1998* (University of Auckland, 1998), 387–392.

[20] T. A. Smith and R. McKibbin, "An investigation of boiling processes in hydrothermal eruptions", *Proc. 21st New Zealand Geothermal Workshop 1999* (University of Auckland, 1999), 229–236.

[21] T. A. Smith and R. McKibbin, "An investigation of boiling processes in hydrothermal eruptions", in: *Proc. World Geothermal Congress 2000,* Tokyo, Japan (eds E. Eglesias, D. Blackwell, T. Hunt, J. Lund, S. Tamanyu and K. Kimbora), (International Geothermal Association, 2000) 699–704.

[22] T. A. Smith and R. McKibbin, "Modelling hydrothermal eruptions", *New Zealand Sci. Review* **60** (2003) 134–136.

[23] K. H. Wohletz and G. A. Valentine, "Computer simulations of explosive volcanic eruptions", in: *Magma transport and strorage* (ed. M. P. Cyan), (Wiley, London, 1990) Chapter 8, 113–135.